Applied Mathematics & Information Sciences
An International Journal

http://dx.doi.org/10.18576/amis/190518

Modeling the Impacts of Water Pollutants on the Dynamics of Aquatic Species Populations

Christopher Ngalya[1,2,*], *Silas Mirau* [1] *and Maranya Mayengo* [1]

[1]School of Computational and Communication Science and Engineering, The Nelson Mandela African Institution of Science and Technology (NM-AIST), P.O. BOX 447 Arusha, Tanzania
[2]Department of ICT and Mathematics, College of Business Education (CBE), P.O. BOX 2077 Dodoma, Tanzania

Received: 7 Jun. 2025, Revised: 21 Jul. 2025, Accepted: 23 Aug. 2025
Published online: 1 Sep. 2025

Abstract: Water pollution poses significant challenges to aquatic ecosystems, affecting the survival of various species. This study formulates a nonlinear mathematical model to examine the interactions among organic pollutants, inorganic pollutants, aquatic plants, bacteria, dissolved oxygen, and the fish populations. The study incorporated aquatic plants into the ecosystem, which had been previously overlooked, and considered more interactions than earlier studies. The model identifies and analyzes four equilibrium points to understand system behavior and stability. Results indicate that inorganic pollutants are strongly linked to the decline of fish populations due to their toxic effects. Conversely, moderate levels of organic pollutants can stimulate the fish population growth by supporting bacterial and plant activity; however, excessive organic pollutants lead to dissolved oxygen depletion, threatening aquatic species. Numerical simulations confirm the local and global stability of the system's interior equilibrium, providing insights into pollutant thresholds that sustain aquatic life. These findings underscore the importance of managing both organic and inorganic pollution to maintain balanced aquatic ecosystems. The results can guide environmental policies on pollutant regulation and biodiversity conservation.

Keywords: Aquatic species, Dissolved oxygen, Mathematical model, Numerical simulation, Pollutants

1 Introduction

Water pollution, caused by both anthropogenic activities and natural processes, continues to pose a significant threat to the rich biodiversity of aquatic ecosystems (1). Pollutants such as toxic chemicals, excess nutrients, sediments, invasive species, and pathogens disrupt the delicate balance of these ecosystems, leading to population declines among aquatic organisms (2). This threat affects a wide range of aquatic species, from fish and amphibians to invertebrates and microorganisms. Their survival and health depend on their ability to adapt to shifting water quality conditions (3; 4). For humans, water pollution has serious health implications, particularly through the contamination of drinking water sources and exposure to hazardous substances (5). Consumption of water containing heavy metals like lead, mercury, and arsenic can result in neurological disorders, developmental delays in children, and chronic kidney diseases (6). Waterborne pathogens—including bacteria, viruses, and parasites—contribute to gastrointestinal diseases, cholera, and typhoid fever, disproportionately affecting communities in regions lacking adequate water treatment infrastructure (7). Long-term exposure to industrial contaminants and agricultural runoff, such as pesticides and nitrates, is associated with increased risks of cancer and endocrine disruption (5). These effects underscore the urgent need for stringent water pollution control strategies to safeguard public health (8). When organic matter enters a water body, it integrates into the aquatic food chain (40). Organic pollution can enrich nutrient availability, fostering microbial growth and potentially benefiting the ecosystem as a whole (41). However, excessive organic loading can lead to eutrophication, hypoxia, and biodiversity loss (42; 43). As the cumulative discharge of organic waste increases, dissolved oxygen levels decline, eventually becoming insufficient to support aquatic life (10). Bacteria and other microorganisms consume oxygen during decomposition, further reducing its availability (9). When surface oxygen

* Corresponding author e-mail: christophern@nm-aist.ac.tz

levels fall, anaerobic organisms migrate upward and degrade waste, producing foul-smelling hydrogen sulfide and increasing water turbidity (36). This process obstructs sunlight penetration, limiting photosynthesis and reducing oxygen and food availability for other species (11). Thus, organic pollutants pose an indirect but serious threat to biodiversity by depleting dissolved oxygen (4; 12; 13).

Inorganic substances represent another major class of water pollutants. Naturally occurring elements such as fluoride, arsenic, and boron are common in aquatic systems (14; 15), while industrial waste introduces heavy metals like mercury, cadmium, chromium, and cyanide (16). These metals may remain suspended or dissolved in water, ultimately accumulating in sediments or entering aquatic food webs through consumption by organisms (17). Over time, this bioaccumulation results in metal-related illnesses, threatening aquatic life due to the toxicity and persistence of these compounds (18). Consequently, inorganic pollutants directly impair the growth and survival of aquatic organisms.

Several historical events underscore the devastating consequences of water pollution. In 1986, an algal bloom triggered by *Gymnodinium breve* in the Gulf of Mexico resulted in the death of 22 million fish (19). Black water events—marked by darkened waters due to excessive organic matter and oxygen depletion—occurred in Australia's Murray River in 2010 (20; 21) and the Katherine River in 1987 (22; 23), causing widespread fish kills. In 2022, severe pollution following flooding in Tanzania's Mara River led to darkened waters and massive aquatic mortality (24). These cases reinforce the need for proactive pollution control to preserve aquatic biodiversity.

Mathematical modeling has emerged as a valuable tool for investigating the impact of pollutants on aquatic ecosystems. The study by (25) analyzed how organic and inorganic pollutants affect fish populations but did not account for the role of aquatic plants in oxygen production. This represents a significant gap, as aquatic plants (invasive species) play a crucial role in enhancing oxygen levels and serving as a food source—an aspect that is addressed in this study by explicitly incorporating aquatic plants into the model. Study by (26) studied oxygen depletion due to algal blooms using a Holling Type-III functional response but focused primarily on nutrient-algae dynamics. The model developed by (4) explored the combined influence of eutrophication and pollution on oxygen dynamics, demonstrating that simultaneous stressors significantly deplete oxygen levels. However, they did not analyze long-term toxic effects on fish. Research by (27) examined toxicant effects on biological populations, emphasizing emission regulation, but lacked consideration of broader ecological and health impacts. The study of (13) developed a nutrient-based species model using nonlinear differential equations but omitted the interaction of pollutants with ecosystem factors. These studies highlight the need for more integrated models that include ecological feedbacks and additional stressors.

This study addresses these limitations by incorporating aquatic plants as a crucial factor in regulating oxygen dynamics. By integrating interactions among pollutants, bacteria, dissolved oxygen, and the fish population, this study presents a more comprehensive perspective on the ecological consequences of water pollution. In doing so, it enhances existing models and offers practical insights for conservation planning and pollution management. The urgency of this topic lies not only in its environmental importance but also in its implications for public health and livelihoods. By closing knowledge gaps and refining predictive capabilities, this research contributes to sustainable ecosystem protection and effective water resource management.

2 Materials and Methods

2.1 Formulation of the Basic Model

This study implements specific modifications to the model proposed by (25) to improve the accuracy of the results. The model is based on the understanding that pollutants entering a water body typically include both organic and inorganic substances (28). To describe the system mathematically, we define several variables: P_o represents the concentration of organic pollutants, and P_i denotes the concentration of inorganic pollutants. Additional variables include B for the population density of bacteria, A for the population density of aquatic plants (such as algae and water hyacinth), C for the concentration of dissolved oxygen, and F for the population density of fish in the water body.

It is assumed that pollutants are discharged into the water body at rates Q_1 and Q_2 for inorganic and organic pollution, respectively. These substances are either flushed out or naturally degraded, with degradation rates denoted by μ_1 for inorganic pollutants and μ_2 for organic pollutants. Bacteria decompose organic pollutants, leading to an increase in their population. In contrast, the uptake of inorganic pollutants by fish adversely affects their growth. Bacteria die at a natural rate μ_6 and undergo intraspecific competition at a rate λ_{20}. Similarly, aquatic plants have a natural mortality rate μ_3 and experience intraspecific competition at a rate λ_{30}.

A constant influx of dissolved oxygen, denoted by Λ, enters the system either from the atmosphere or through photosynthesis by aquatic plants. This oxygen supply diminishes over time at a natural depletion rate μ_4. Additionally, dissolved oxygen aids in the decomposition of dead bacteria into organic matter at a rate of β_{02}.

According to (29), fish population growth is entirely dependent on the availability of dissolved oxygen. Fish are affected in two ways when exposed to pollution: inorganic pollutants directly suppress growth, while organic pollutants reduce oxygen availability, indirectly impairing growth. Fish experience natural mortality at a rate μ_5, intraspecific competition at a rate λ_{10}, and pollution-induced mortality from ingestion of inorganic toxins at a rate θ.

We adopt the Monod-type interaction as employed by (30) and (4), which describes species growth in response to nutrient concentration. The cumulative depletion of organic pollutants P_o by bacterial consumption is given by the expression $\frac{\beta_{20}P_oB}{\beta_{21}+\beta_{22}P_o}$. Organic pollutants are also consumed by fish and aquatic plants at rates $\frac{k_1P_oF}{k_{12}+k_{11}P_o}$ and $\frac{\beta_{01}P_oA}{\beta_{12}+\beta_{11}P_o}$, respectively.

Using the same Monod formulation, aquatic plants benefit from consuming P_o at a rate of $\frac{\lambda_3\beta_{01}P_oA}{\beta_{12}+\beta_{11}P_o}$, while bacteria gain at a rate of $\frac{\lambda_2\beta_{20}P_oB}{\beta_{21}+\beta_{22}P_o}$. During the decomposition of organic matter, dissolved oxygen is depleted at a rate of $\frac{\beta_{02}P_oB}{\beta_{21}+\beta_{22}P_o}$. Additionally, fish benefit nutritionally by consuming P_o at a rate of $\frac{\lambda_4k_1P_oF}{k_{12}+k_{11}P_o}$.

Based on these dynamics, we formulate the model as a system of nonlinear differential equations, presented in Eq. (1) below.

$$\begin{cases} \frac{dP_i}{dt} = Q_1 - \alpha P_iF - \mu_1P_i \\ \frac{dP_o}{dt} = Q_2 - \frac{\beta_{20}P_oB}{\beta_{21}+\beta_{22}P_o} - \frac{k_1P_oF}{k_{12}+k_{11}P_o} - \frac{\beta_{01}P_oA}{\beta_{12}+\beta_{11}P_o} \\ \qquad -\mu_2P_o \\ \frac{dA}{dt} = \Lambda_2A + \frac{\lambda_3\beta_{01}P_oA}{\beta_{12}+\beta_{11}P_o} - \mu_3A - \lambda_{30}A^2 \\ \frac{dB}{dt} = \Lambda_3B + \frac{\lambda_2\beta_{20}P_oB}{\beta_{21}+\beta_{22}P_o} - \mu_6B - \lambda_{20}B^2 \\ \frac{dC}{dt} = \Lambda - \frac{\beta_{02}P_oB}{\beta_{21}+\beta_{22}P_o} - \gamma_1CF - \gamma_2A - \gamma_3B - \mu_4C \\ \frac{dF}{dt} = \Lambda_1F + \frac{\lambda_4k_1P_oF}{k_{12}+k_{11}P_o} + \gamma_1CF - \theta P_iF - \mu_5F - \lambda_{10}F^2 \end{cases} \tag{1}$$

with initial conditions, $P_i(0) > 0, P_o(0) > 0, B(0) > 0, A(0) > 0, F(0) > 0, C(0) > 0$.

2.2 Qualitative Analysis

2.2.1 Boundness of the model

The model system (1) was developed taking into account the fields of Biology, Environment, Epidemiology, and Ecology assuming that all the state variables and model parameters are well–posed for all $t \geq 0$. Initially, we demonstrate that the solutions of the model (1) are bounded.

Lemma 1. *The region of attraction for the model system (1) is contained in the following set:*

$$\Omega = \left\{ (P_i, P_o, A, B, C, F) \in \mathbb{R}^6_+ : 0 \leq P_i \leq \frac{Q_1}{\mu_1}, 0 \leq P_o \leq \frac{Q_2}{\mu_2}, \right.$$
$$\left. 0 \leq A \leq L_A, 0 \leq B \leq L_B, 0 \leq C \leq \frac{\Lambda}{\mu_4}, 0 \leq F \leq L_F \right\},$$

where

$$L_A = \frac{1}{\lambda_{30}}\left[\Lambda_2 - \mu_3 + \frac{\lambda_3\beta_{01}Q_2}{\mu_2\beta_{12}+\beta_{11}Q_2}\right],$$

$$L_B = \frac{1}{\lambda_{20}}\left[\Lambda_3 - \mu_7 + \frac{\lambda_2\beta_{20}Q_2}{\mu_2\beta_{21}+\beta_{22}Q_2}\right],$$

$$L_F = \left[\frac{\lambda_4k_1Q_2}{\lambda_{10}(\mu_2k_{12}+k_{11}Q_2)} + \frac{\Lambda_1\mu_1 + \gamma_1L_C\mu_1 - \mu_5\mu_1}{\lambda_{10}\mu_1}\right].$$

Proof. Following (31), we will prove this lemma. From the first equation of model system (1), we establish that,

$$\frac{dP_i}{dt} \leq Q_1 - \mu_1P_i, \tag{2}$$

whose solution is given by

$$\limsup_{t\to\infty} P_i \leq \frac{Q_1}{\mu_1}.$$

Therefore, we have

$$0 \leq P_i \leq \frac{Q_1}{\mu_1}. \tag{3}$$

2.3 Positivity of the model solution

For the model system (1) to be ecologically and mathematically meaningful, we need to prove that all state variables are non-negative for all $t \geq 0$.

Lemma 2. *The solutions $(P_i(t), P_o(t), A(t), B(t), C(t), F(t))$ of model system (1) with initial conditions $P_i(0) > 0, P_o(0) > 0, A(0) > 0, B(0) > 0, C(0) > 0$ and $F(0) > 0$ are positive for all $t \geq 0$.*

Proof. Considering the first equation of model system (1), we have

$$\frac{dP_i}{dt} > -(\alpha F + \mu_1)P_i, \tag{4}$$

whose solution is given by

$$P_i(t) > P_i(0)e^{-(\alpha F+\mu_1)t}.$$

Likewise, the variables $P_o(t), A(t), B(t), C(t)$ and $F(t)$ can be computed following similar procedure and establish that $P_o(t) > 0, B(t) > 0, A(t) > 0, F(t) > 0, C(t) > 0$ whenever $t \geq 0$. Therefore the solution set $(P_i(t), P_o(t), A(t), B(t), C(t), F(t)) \in \mathbb{R}^6_+, \forall t \geq 0$.

2.4 Analysis of Equilibrium Points

To understand the long-term behavior of the model system, we first identify equilibrium solutions and then examine their stability properties. The equilibrium points represent steady-state solutions of the formulated model system, where the growth rates of all dynamical variables are set to zero.

2.4.1 Possible equilibrium points

The model system (1), has at least four viable equilibrium points, outlined as follows:

i. $E_0 = (0,0,0,0,0,0)$, in this equilibrium point we assumes water have no pollutions, no aquatic plants, no bacteria, no oxygen and no fish.
ii. $E_1 = \left(\frac{Q_1}{\mu_1}, \frac{Q_2}{\mu_2}, 0, 0, \frac{\Lambda}{\mu_4}, 0\right)$, expresses the absence of aquatic plants, bacteria and fish in the system.
iii. $E_2 = (0,0,A_2,B_2,C_2,F_2)$, expresses the absence of pollutant materials in the water body.
iv. $E^* = (P_i^*, P_o^*, A^*, B^*, C^*, F^*)$, expresses the co-existence of all the species in the system.

While the existence of E_0 and E_1 is trivial, and occur with no conditions; the equilibria E_2 and E^* are nontrivial and may require some established conditions for their existence.

2.4.2 Existance Pollutants Free Equilibrium Point (E_2)

The pollutant-free equilibrium point E_2 is obtained by solving the following reduced system:

$$\begin{cases} (\Lambda_2 - \mu_3 - \lambda_{30}A_2)A_2 = 0 \\ (\Lambda_3 - \mu_6 - \lambda_{20}B_2)B_2 = 0 \\ \Lambda - \gamma_1 C_2 F_2 - \gamma_2 A_2 - \gamma_3 B_2 - \mu_4 C_2 = 0 \\ (\Lambda_1 + \gamma_1 C_2 - \mu_5 - \lambda_{10}F_2)F_2 = 0 \end{cases} \tag{5}$$

The first two equations yield the expressions $A_2 = \frac{\Lambda_2 - \mu_3}{\lambda_{30}}$ and $B_2 = \frac{\Lambda_3 - \mu_6}{\lambda_{20}}$, provided $A_2, B_2 \neq 0$. From the fourth equation, when $F_2 \neq 0$, we obtain:

$$F_2 = \frac{(\Lambda_1 - \mu_5) + \gamma_1 C_2}{\lambda_{10}} \triangleq f_1(C_2) \tag{6}$$

Substituting A_2, B_2, and $f_1(C_2)$ into the third equation of system (5), we define the function $f_2(C_2)$ as:

$$\begin{aligned} f_2(C_2) = \Lambda - \gamma_1 C_2 f_1(C_2) - \gamma_2 \left(\frac{\Lambda_2 - \mu_3}{\lambda_{30}}\right) \\ - \gamma_3 \left(\frac{\Lambda_3 - \mu_6}{\lambda_{20}}\right) - \mu_4 C_2 = 0 \end{aligned} \tag{7}$$

The following observations are made:

i. $f_2(0) = \Lambda - \gamma_2 \left(\frac{\Lambda_2 - \mu_3}{\lambda_{30}}\right) - \gamma_3 \left(\frac{\Lambda_3 - \mu_6}{\lambda_{20}}\right) > 0$ if

$$0 < \gamma_2 \left(\frac{\Lambda_2 - \mu_3}{\lambda_{30}}\right) + \gamma_3 \left(\frac{\Lambda_3 - \mu_6}{\lambda_{20}}\right) < \Lambda$$

ii. $f_2\left(\frac{\Lambda}{\mu_4}\right) < 0$
iii. $f_2'(C_2) = -\gamma_1 f_1(C_2) - \gamma_1 C_2 f_1'(C_2) - \mu_4 < 0$

These considerations suggest that $f_2(C_2)$ admits a unique positive root in the interval $0 < C_2 < \frac{\Lambda}{\mu_4}$. Hence, the equilibrium point

$$E_2 = (0,0,A_2,B_2,C_2,F_2)$$

exists under the following conditions:

$$\begin{cases} \Lambda_2 - \mu_3 > 0 \\ \Lambda_3 - \mu_6 > 0 \\ \Lambda_1 - \mu_5 > 0 \\ 0 < \gamma_2 \left(\frac{\Lambda_2 - \mu_3}{\lambda_{30}}\right) + \gamma_3 \left(\frac{\Lambda_3 - \mu_6}{\lambda_{20}}\right) < \Lambda \end{cases} \tag{8}$$

2.4.3 Existence of Interior Equilibrium Point (E^*)

The interior critical point E^* is obtained by solving the following simultaneous equations:

$$\begin{cases} 0 = Q_1 - \alpha P_i^* F^* - \mu_1 P_i^* \\ 0 = Q_2 - \dfrac{\beta_{20} P_o^* B^*}{\beta_{21}+\beta_{22}P_o^*} - \dfrac{k_1 P_o^* F^*}{k_{12}+k_{11}P_o^*} \\ \quad - \dfrac{\beta_{01} P_o^* A^*}{\beta_{12}+\beta_{11}P_o^*} - \mu_2 P_o^* \\ 0 = \Lambda_2 A^* + \dfrac{\lambda_3 \beta_{01} P_o^* A^*}{\beta_{12}+\beta_{11}P_o^*} - \mu_3 A^* - \lambda_{30} A^{*2} \\ 0 = \Lambda_3 B^* + \dfrac{\lambda_2 \beta_{20} P_o^* B^*}{\beta_{21}+\beta_{22}P_o^*} - \mu_6 B^* - \lambda_{20} B^{*2} \\ 0 = \Lambda - \dfrac{\beta_{02} P_o^* B^*}{\beta_{21}+\beta_{22}P_o^*} - \gamma_1 C^* F^* - \gamma_2 A^* - \gamma_3 B^* \\ \quad - \mu_4 C^* \\ 0 = \Lambda_1 F^* + \dfrac{\lambda_4 k_1 P_o^* F^*}{k_{12}+k_{11}P_o^*} + \gamma_1 C^* F^* - \theta P_i^* F^* \\ \quad - \mu_5 F^* - \lambda_{10} F^{*2} \end{cases} \tag{9}$$

when all the variables are positive. From the first equation, we establish P_i^* as a function of F^* such that,

$$P_i^* = \frac{Q_1}{\alpha F^* + \mu_1} = f_3(F^*) \tag{10}$$

$$A^* = \left(\frac{\Lambda_2 - \mu_3}{\lambda_{30}} - \frac{\lambda_3 \beta_{01} P_o^*}{\lambda_{30}(\beta_{12}+\beta_{11}P_o^*)}\right) = f_4(P_o^*), \tag{11}$$

$$B^* = \left(\frac{\Lambda_3 - \mu_6}{\lambda_{20}} - \frac{\lambda_3 \beta_{02} P_o^*}{\lambda_{20}(\beta_{21}+\beta_{22}P_o^*)}\right) = f_5(P_o^*), \tag{12}$$

$$C^* = \frac{1}{\gamma_1 F^* - \mu_4}\left(\Lambda - \frac{\beta_{02} P_o^* f_5(P_o^*)}{\beta_{21}+\beta_{22}P_o^*} - \gamma_2 f_4(P_o^*) - \gamma_3 f_5(P_o^*)\right) = f_6(P_o^*, F^*). \tag{13}$$

After proper substitution the isoclines 14 and 15 are established.

$$Q_2 - \frac{\beta_{20} P_o^* f_5(P_o^*)}{\beta_{21}+\beta_{22}P_o^*} - \frac{k_1 P_o^* F^*}{k_{12}+k_{11}P_o^*} - \frac{\beta_{01} P_o^* f_4(P_o^*)}{\beta_{12}+\beta_{11}P_o^*} - \mu_2 P_o^* = f_7(P_o^*, F^*). \tag{14}$$

$$(\Lambda_1 - \mu_5) + \frac{\lambda_4 k_1 P_o^*}{k_{12}+k_{11}P_o^*} + \gamma_1 f_6(P_o^*, F^*) - \theta f_3(F^*) - \lambda_{10} F^* = f_8(P_o^*, F^*). \tag{15}$$

From the isocline (14) we infer the following:

1.When $F^* = 0$, we have $f_7(P_o^*, 0) = g_1(P_o^*)$ (say), where

$$Q_2 - \frac{\beta_{20} P_o^* f_5(P_o^*)}{\beta_{21}+\beta_{22}P_o^*} - \frac{\beta_{01} P_o^* f_4(P_o^*)}{\beta_{12}+\beta_{11}P_o^*} - \mu_2 P_o^* = g_1(P_o^*) \tag{16}$$

(a)When $P_o^* = 0$, we have $g_1(0) = Q_2 > 0$.

(b)When $P_o^* = \dfrac{Q_2}{\mu_2}$, we have

$$g_1\left(\frac{Q_2}{\mu_2}\right) = -\left[\frac{\beta_{20}\left(\frac{Q_2}{\mu_2}\right) f_5\left(\frac{Q_2}{\mu_2}\right)}{\beta_{21}+\beta_{22}\left(\frac{Q_2}{\mu_2}\right)} + \frac{\beta_{01}\left(\frac{Q_2}{\mu_2}\right) f_4\left(\frac{Q_2}{\mu_2}\right)}{\beta_{12}+\beta_{11}\left(\frac{Q_2}{\mu_2}\right)}\right] < 0.$$

(c)After performing the necessary computations and simplifications, it can be demonstrated that $g_1'(P_o^*) < 0$ provided that inequality (17) is satisfied:

$$\frac{\beta_{20} P_o^* f_4(P_o^*) \beta_{22}}{(\beta_{21}+\beta_{22}P_o^*)^2} + \frac{\beta_{01} P_o^* f_3(P_o^*) \beta_{11}}{(\beta_{12}+\beta_{11}P_o^*)^2} < \frac{\beta_{20} f_4(P_o^*) + \beta_{20} P_o^* f_4'(P_o^*)}{\beta_{21}+\beta_{22}P_o^*} + \frac{\beta_{01} f_3(P_o^*) + \beta_{01} P_o^* f_3'(P_o^*)}{\beta_{12}+\beta_{11}P_o^*} + \mu_2. \tag{17}$$

The relationships established in (a)–(c) above confirm that equation (16) has a unique positive solution with

$$0 < P_o^* < \frac{Q_2}{\mu_2}.$$

2.When $F^* \to \infty$, we find that $\left(\dfrac{dP_o^*}{dF^*}\right)_1 < 0$.

From the isocline (15) the following results are established

1.When $F^* = 0$, gives $f_3(P_o^*, 0) = g_2(P_0^*)$ (say).

$$(\Lambda_1 - \mu_5) + \frac{\lambda_4 k_1 P_o^*}{k_{12} n + k_{11} P_o^*} + \gamma_1 f_6(P_o^*) - \frac{\theta Q_1}{\mu_1} = g_2(P_o^*). \tag{18}$$

(a)When $P_o^* = 0$, gives $g_2(0) < 0$, provided that inequality (19) holds

$$(\Lambda_1 - \mu_5) + \gamma_1 f_6(0) < \frac{\theta Q_1}{\mu_1}. \quad (19)$$

(b)When $P_o^* = \frac{Q_2}{\mu_2}$, gives $g_2\left(\frac{Q_2}{\mu_2}\right) > 0$ provided that inequality (20) holds.

$$(\Lambda_1 - \mu_5) + \frac{\lambda_4 k_1 \left(\frac{Q_2}{\mu_2}\right)}{k_{12} + k_{11}\left(\frac{Q_2}{\mu_2}\right)} + \gamma_1 f_6\left(\frac{Q_2}{\mu_2}\right) > \frac{\theta Q_1}{\mu_1}. \quad (20)$$

(c)The derivative of $g_2(P_o^*)$ with respect to P_o^* gives,

$$g_2'(P_o^*) = \frac{\lambda_4 k_{11} k_{12}}{(k_{11}P_o^* + k_{12})^2} + \gamma_1 f_6'(P_o^*) > 0$$

.

Considerations (*a*-*c*), we noted that (15) has a positive unique solution in $0 < P_o^* < \frac{Q_2}{\mu_2}$.

2. $\left(\frac{dP_o^*}{dF^*}\right)_2 > 0.$

Therefore, the values of P_o^* and F^* are unique (see Fig. 1) in the regions $0 < P_o < L_{P_o}$ and $0 < F < L_F$, respectively, provided $\left(\frac{dP_o}{dF}\right)_1 < 0$ and $\left(\frac{dP_o}{dF}\right)_2 > 0$.

Once the values of P_o^* and F^* are determined, the values of P_i^*, A^*, B^* and C^* can be evaluated from equations (10), (11), (12) and (13), respectively.

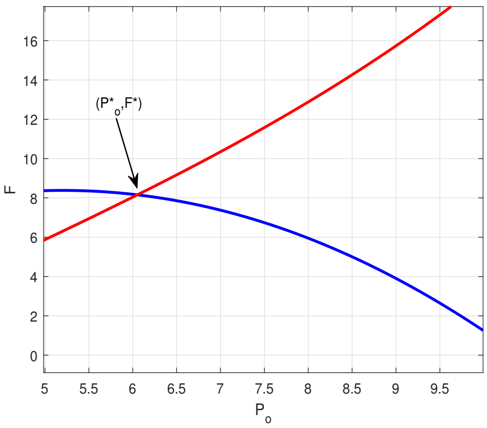

Fig. 1: The plot to illustrates the intersection of isoclines (14) and (15), highlighting an existence of (P_o^*, F^*) within the interior of the first quadrant.

2.5 Stability Analysis

2.5.1 Stability Analysis of Equilibrium Points

The stability of the equilibrium points E_0, E_1, and E_2 of the model system (1) is analyzed using the *eigenvalue method*, whereas the stability of the interior equilibrium point E^* is evaluated using an appropriate *Lyapunov candidate function*. The general Jacobian matrix J of the model system (1) is given by:

$$J = \begin{bmatrix} J_{11} & 0 & 0 & 0 & 0 & J_{16} \\ 0 & J_{22} & J_{23} & J_{24} & 0 & J_{26} \\ 0 & J_{32} & J_{33} & 0 & 0 & 0 \\ 0 & J_{42} & 0 & J_{44} & 0 & 0 \\ 0 & J_{52} & J_{53} & J_{54} & J_{55} & J_{56} \\ J_{61} & J_{62} & 0 & 0 & J_{65} & J_{66} \end{bmatrix} \quad (21)$$

where the entries are defined as:

$$J_{11} = -\alpha F - \mu_1, \quad J_{16} = -\alpha P_i,$$

$$J_{22} = -\frac{\beta_{20}B}{\beta_{22}P_o + \beta_{21}} + \frac{\beta_{20}P_o B\beta_{22}}{(\beta_{22}P_o + \beta_{21})^2} - \frac{k_1 F}{k_{11}P_o + k_{12}} + \frac{k_1 P_o F k_{11}}{(k_{11}P_o + k_{12})^2} - \frac{\beta_{01}A}{\beta_{11}P_o + \beta_{12}} + \frac{\beta_{01}P_o A\beta_{11}}{(\beta_{11}P_o + \beta_{12})^2} - \mu_2,$$

$$J_{23} = -\frac{\beta_{01}P_o}{\beta_{12} + \beta_{11}P_o}, \quad J_{24} = -\frac{\beta_{20}P_o}{\beta_{21} + \beta_{22}P_o},$$

$$J_{26} = -\frac{k_1 P_o}{k_{12} + k_{11}P_o}, \quad J_{32} = \frac{\lambda_3\beta_{01}A\beta_{12}}{(\beta_{11}P_o + \beta_{12})^2},$$

$$J_{33} = \Lambda_2 - \mu_3 + \frac{\lambda_3\beta_{01}P_o}{\beta_{12} + \beta_{11}P_o} - 2\lambda_{30}A,$$

$$J_{42} = \frac{\beta_{20}B\lambda_2\beta_{21}}{(\beta_{22}P_o + \beta_{21})^2},$$

$$J_{44} = \Lambda_3 - \mu_6 - \frac{\beta_{02}P_o B}{\beta_{21} + \beta_{22}P_o} - 2\lambda_{20}B,$$

$$J_{52} = -\frac{\beta_{02}B\beta_{21}}{(\beta_{22}P_o + \beta_{21})^2}, \quad J_{53} = -\gamma_2,$$

$$J_{54} = -\gamma_3, \quad J_{55} = \gamma_2 - \gamma_1 F - \gamma_3 - \mu_5,$$

$$J_{56} = -\gamma_1 C, \quad J_{61} = \theta F,$$

$$J_{62} = \frac{\lambda_4 k_1 F k_{12}}{(k_{11}P_o + k_{12})^2}, \quad J_{65} = \gamma_1 F,$$

$$J_{66} = \Lambda_1 - \mu_5 + \frac{\lambda_4 k_1 P_o}{k_{12} + k_{11}P_o} + \gamma_1 C - \theta P_i - 2\lambda_{10}F.$$

2.5.2 Stability of Trivial Equilibrium Point

Eigenvalues of the Jacobian matrix J evaluated at Trivial Equilibrium Point, E_0 are $-\mu_1,\ -\mu_2,\ (\Lambda_2-\mu_3),\ (\Lambda_3-\mu_6),\ \gamma_2-\gamma_3-\mu_5$ and $(\Lambda_1-\mu_5)$. Conditions (8) show that eigenvalues $(\Lambda_2-\mu_3)>0$ and $(\Lambda_3-\mu_6)>0$ respectively, suggesting instability of equilibrium point E_0.

2.5.3 Stability of Bacteria-Plants and Fish Free Equilibrium Point E_1

Eigenvalues of the Jacobian matrix J evaluated at the Bacteria-Plants and Fish Free Equilibrium Point, E_1 are $-\mu_1, -\mu_2, (\Lambda_2-\mu_3)+\dfrac{\lambda_3\beta_{01}Q_2}{\beta_{12}\mu_2+\beta_{11}Q_2}, (\Lambda_3-\mu_6), (\gamma_2-\mu_5)-\gamma_3$, and $(\Lambda_1-\mu_5)+\dfrac{\lambda_4 k_1 Q_2}{k_{12}\mu_2+k_{11}Q_2}+\gamma_1 C-\dfrac{\theta Q_1}{\mu_1}$. Conditions (8) show that eigenvalues $(\Lambda_2-\mu_3)+\dfrac{\lambda_3\beta_{01}Q_2}{\beta_{12}\mu_2+\beta_{11}Q_2}>0$ and $\Lambda_3-\mu_6>0$ which confirm that equilibrium point E_1 is unstable.

2.5.4 Stability of Pollutants Free Equilibrium Point

Eigenvalues of the Jacobian matrix J evaluated at the Pollutants free equilibrium point The eigenvalues at the equilibrium point E_2 are given by:

$$
-(\alpha_1F_2+\mu_1), \qquad -\left(\frac{\beta_{20}B_2}{\beta_{21}}+\frac{k_1F_2}{k_{12}}+\frac{\beta_{01}A_2}{\beta_{12}}+\mu_2\right),
$$
$$
(\Lambda_2-\mu_3)-2\lambda_{30}A_2, \qquad (\Lambda_3-\mu_6)-2\lambda_{20}B_2,
$$
$$
(\gamma_2-\mu_5)-(\gamma_1F_2+\gamma_3), \qquad -\gamma_1C_2,
$$
$$
\gamma_1F_2, \qquad (\Lambda_1-\mu_5)+\gamma_1C_2-2\lambda_{10}F_2.
$$

Since $\gamma_1F_2>0,\ldots$ the equilibrium E_2 is unstable.

2.5.5 Stability of an Interior Equilibrium Point (E^*)

Theorems 1 and 26 establish the conditions for local and global stability of equilibrium point E^* respectively.

Theorem 1. *The equilibrium E^*, is locally asymptotically stable if the following conditions hold:*

$$
\begin{cases}
(\alpha F^*+\mu_1)\left(\theta P_i^*+\mu_5+2\lambda_{10}F^*-\Lambda_1 \right. \\
\qquad \left. -\dfrac{\lambda_4k_1P_o^*}{k_{12}+k_{11}P_o^*}+\gamma_1C^*\right)>(\mu_1P_i^*-m_5\theta F^*)^2, \\
m_2\left(\mu_3+2\lambda_{30}A^*-\Lambda_2-\dfrac{\lambda_3\beta_1P_o^*}{\beta_{12}+\beta_{11}P_o^*}\right)(\gamma_1F^*+\gamma_3) \\
\qquad >\dfrac{P_o^*(k_{11}P_o^*+k_{12})}{\lambda_4\gamma_1k_{12}C^*}\gamma_2^2, \\
\left(\dfrac{\beta_{02}P_o^*B^*}{\beta_{21}+\beta_{22}P_o^*}+\mu_6+2\lambda_{20}B^*-\Lambda_3\right)(\mu_5-\gamma_2) \\
\qquad >\dfrac{P_o^*(k_{11}P_o^*+k_{12})}{\lambda_4\gamma_1k_{12}C^*}\gamma_3^2.
\end{cases} \tag{22}
$$

Proof. Following (32), we study the behavior of the system in the neighborhood of equilibrium point when given a small perturbation. We first linearlize the system using the following transformations: $P_i=P_i^*+p_i; P_o=P_o^*+p_o; A=A^*+a; B=B^*+b; C=C^*+c; F=F^*+f$, where p_i, p_o, a, b, c, and f are small perturbations around the equilibrium.
The linearlized system is given by

$$
\begin{aligned}
\frac{dp_i}{dt} &= (-\alpha F^*-\mu_1)p_i-\mu_1P_i^*f, \\
\frac{dp_o}{dt} &= \left(\frac{\beta_{20}\beta_{22}P_o^*B^*}{(\beta_{22}P_o^*+\beta_{21})^2}-\frac{\beta_{20}B^*}{\beta_{22}P_o^*+\beta_{21}}-\frac{k_1F^*}{k_{11}P_o^*+k_{12}}+\frac{k_1k_{11}P_o^*F^*}{(k_{11}P_o^*+k_{12})^2}\right. \\
&\quad \left.-\frac{\beta_{01}A^*}{\beta_{11}P_o^*+\beta_{12}}\right)p_o-\left(\frac{\beta_{01}P_o^*}{\beta_{12}+\beta_{11}P_o^*}\right)a-\left(\frac{\beta_{20}P_o^*}{\beta_{21}+\beta_{22}P_o^*}\right)b \\
&\quad -\left(\frac{k_1P_o^*}{k_{12}+k_{11}P_o^*}\right)f, \\
\frac{da}{dt} &= \left(\frac{\lambda_3\beta_1\beta_{12}A^*}{(\beta_{11}P_o^*+\beta_{12})^2}\right)p_o+\left(\Lambda_2+\frac{\lambda_3\beta_1P_o^*}{\beta_{12}+\beta_{11}P_o^*}-\mu_3-2\lambda_{30}A^*\right)a, \\
\frac{db}{dt} &= \left(\frac{\lambda_2\beta_{20}\beta_{21}B^*}{(\beta_{22}P_o^*+\beta_{21})^2}\right)p_o+\left(\Lambda_3-\frac{\beta_{02}P_o^*B^*}{\beta_{21}+\beta_{22}P_o^*}-\mu_6-2\lambda_{20}B^*\right)b, \\
\frac{dc}{dt} &= -\left(\frac{\beta_{02}\beta_{21}B^*}{(\beta_{22}P_o^*+\beta_{21})^2}\right)p_o-\gamma_2a-\gamma_3b+(\gamma_2-\gamma_1F^*-\gamma_3-\mu_5)c-\gamma_1C^*f, \\
\frac{df}{dt} &= \theta F^*p_i+\left(\frac{\lambda_4k_1k_{12}F^*}{(k_{11}P_o^*+k_{12})^2}\right)p_o+\gamma_1F^*c \\
&\quad +\left(\Lambda_1+\frac{\lambda_4k_1P_o^*}{k_{12}+k_{11}P_o^*}+\gamma_1C^*-\theta P_i^*-\mu_5-2\lambda_{10}F^*\right)f.
\end{aligned} \tag{23}
$$

Now, we consider the following positive definite function:

$$W=\frac{1}{2}\left(p_i^2+m_1p_o^2+\frac{m_2a^2}{A^*}+\frac{m_3b^2}{B^*}+m_4c^2+\frac{m_5f^2}{F^*}\right)$$

where $m_i>0,\quad i=1,\ldots,5,$

and use a linearized model (23) to get

$$\begin{aligned}\frac{dW}{dt}&=-(\alpha F^*+\mu_1)p_i^2\\&-\left(\frac{m_1\beta_{01}A^*}{\beta_{11}P_o^*+\beta_{12}}+\frac{m_1\beta_{20}B^*}{\beta_{22}P_o^*+\beta_{21}}+\frac{m_1k_1F^*}{k_{11}P_o^*+k_{12}}\right)p_o^2\\&+\left(\frac{m_1\beta_{20}\beta_{22}P_o^*B^*}{(\beta_{22}P_o^*+\beta_{21})^2}+\frac{m_1k_1k_{11}P_o^*F^*}{(k_{11}P_o^*+k_{12})^2}\right)p_o^2\\&-m_2\left(\mu_3+2\lambda_{30}A^*-\Lambda_2-\frac{\lambda_3\beta_1P_o^*}{\beta_{12}+\beta_{11}P_o^*}\right)a^2\\&-m_3\left(\frac{\beta_{02}P_o^*B^*}{\beta_{21}+\beta_{22}P_o^*}+\mu_6+2\lambda_{20}B^*-\Lambda_3\right)b^2\\&-m_4(\gamma_1F^*+\gamma_3+\mu_5-\gamma_2)c^2\\&-m_5\left(\theta P_i^*+\mu_5+2\lambda_{10}F^*-\Lambda_1-\frac{\lambda_4k_1P_o^*}{k_{12}+k_{11}P_o^*}\right.\\&\left.\quad-\gamma_1C^*\right)f^2-(\mu_1P_i^*-m_5\theta F^*)p_if\\&-\left(\frac{m_2\lambda_3\beta_1\beta_{12}A^*}{(\beta_{11}P_o^*+\beta_{12})^2}-\frac{m_1\beta_{01}P_o^*}{\beta_{12}+\beta_{11}P_o^*}\right)p_oa\\&-\left(\frac{m_1\beta_{20}P_o^*}{\beta_{21}+\beta_{22}P_o^*}-\frac{m_3\lambda_2\beta_{20}\beta_{21}B^*}{(\beta_{22}P_o^*+\beta_{21})^2}\right)p_ob\\&-m_4\left(\frac{\beta_{02}\beta_{21}B^*}{(\beta_{22}P_o^*+\beta_{21})^2}\right)p_oc.\end{aligned}\tag{24}$$

Choosing the values

$$\begin{aligned}m_1&=1,\\m_2&=-\frac{m_1P_o^*(\beta_{11}P_o^*+\beta_{12})}{\lambda_3\beta_{12}A^*},\\m_3&=\frac{m_1P_o^*(\beta_{22}P_o^*+\beta_{21})}{\lambda_2\beta_{21}B^*},\\m_4&=\frac{m_1P_o^*(k_{11}P_o^*+k_{12})}{\lambda_4\gamma_1k_{12}C^*},\\m_5&=\frac{m_1P_o^*(k_{11}P_o^*+k_{12})}{\lambda_4k_{12}F^*}.\end{aligned}$$

as arbitrary constants, the time derivative of W becomes

$$\begin{aligned}\frac{dW}{dt}=-\Bigg[&(\alpha F^*+\mu_1)p_i^2+\left(\frac{\beta_{20}B^*}{\beta_{22}P_o^*+\beta_{21}}+\frac{k_1F^*}{k_{11}P_o^*+k_{12}}\right.\\&\left.+\frac{\beta_{01}A^*}{\beta_{11}P_o^*+\beta_{12}}-\frac{\beta_{20}\beta_{22}P_o^*B^*}{(\beta_{22}P_o^*+\beta_{21})^2}-\frac{k_1k_{11}P_o^*F^*}{(k_{11}P_o^*+k_{12})^2}\right)p_o^2\\&+m_2\left(\mu_3+2\lambda_{30}A^*-\Lambda_2-\frac{\lambda_3\beta_1P_o^*}{\beta_{12}+\beta_{11}P_o^*}\right)a^2\\&+m_3\left(\frac{\beta_{02}P_o^*B^*}{\beta_{21}+\beta_{22}P_o^*}+\mu_6+2\lambda_{20}B^*-\Lambda_3\right)b^2\\&+m_4(\gamma_1F^*+\gamma_3+\mu_5-\gamma_2)c^2\\&+m_5\left(\theta P_i^*+\mu_5+2\lambda_{10}F^*-\Lambda_1-\frac{\lambda_4k_1P_o^*}{k_{12}+k_{11}P_o^*}+\gamma_1C^*\right)f^2\\&+(\mu_1P_i^*-m_5\theta F^*)p_if-m_4\gamma_2ac-m_4\gamma_3bc\Bigg].\end{aligned}$$

Sufficient conditions for $\frac{dW}{dt}$ to be negative definite obtained by Sylvester's conditions criteria are:

$$\begin{aligned}&(\alpha F^*+\mu_1)\left(\theta P_i^*+\mu_5+2\lambda_{10}F^*-\Lambda_1\right.\\&\qquad\left.-\frac{\lambda_4k_1P_o^*}{k_{12}+k_{11}P_o^*}+\gamma_1C^*\right)>(\mu_1P_i^*-m_5\theta F^*)^2,\\&m_2\left(\mu_3+2\lambda_{30}A^*-\Lambda_2-\frac{\lambda_3\beta_1P_o^*}{\beta_{12}+\beta_{11}P_o^*}\right)(\gamma_1F^*+\gamma_3)\\&\qquad>\frac{P_o^*(k_{11}P_o^*+k_{12})}{\lambda_4\gamma_1k_{12}C^*}\gamma_2^2,\\&\left(\frac{\beta_{02}P_o^*B^*}{\beta_{21}+\beta_{22}P_o^*}+\mu_6+2\lambda_{20}B^*-\Lambda_3\right)(\mu_5-\gamma_2)\\&\qquad>\frac{P_o^*(k_{11}P_o^*+k_{12})}{\lambda_4\gamma_1k_{12}C^*}\gamma_3^2.\end{aligned}\tag{25}$$

From these inequalities, we can choose a positive value m_2, provided that inequality (25) holds. Thus the time-derivative of W is negative definite and this result demonstrates the stability of the coexistence equilibrium.

Theorem 2. *The interior equilibrium E^*, if exists, is non-linearly stable inside the region of attraction if the following conditions hold:*

$$m_5\theta^2<\lambda_{10}(\mu_1-\alpha L_F),$$

$$\left(\frac{m_2\lambda_3\beta_1\beta_{12}}{(\beta_{12}+\beta_{11}P_o^*)(\beta_{12}+\beta_{11}L_{P_o})}\right)^2<\frac{m_1\lambda_{30}\beta_{20}\beta_{21}L_B}{(\beta_{21}+\beta_{22}P_o^*)(\beta_{21}+\beta_{22}L_{P_o})},$$

$$\left(\frac{m_3\lambda_2\beta_{20}\beta_{21}}{(\beta_{21}+\beta_{22}P_o^*)(\beta_{21}+\beta_{22}L_{P_o})}\right)^2$$

$$< \frac{m_1\lambda_{20}k_1k_{12}L_F}{(k_{12}+k_{11}P_o^*)(k_{12}+k_{11}L_{P_o})},$$

$$m_4\left(\frac{\beta_{20}\beta_{21}L_B}{(\beta_{21}+\beta_{22}P_o^*)(\beta_{21}+\beta_{22}L_{P_o})}\right)^2$$

$$< \frac{(\gamma_1L_F-\gamma_4)m_1\beta_{01}\beta_{12}L_B}{(\beta_{12}+\beta_{11}P_o^*)(\beta_{12}+\beta_{11}L_{P_o})},$$

$$m_5\left(\frac{k_1k_{12}}{(k_{12}+k_{11}P_o^*)(k_{12}+k_{11}L_{P_o})}\right)^2 < \lambda_{10}\mu_2,$$

$$m_4\gamma_2^2 < \lambda_{30}(\gamma_1L_F-\gamma_4),$$

$$m_5\gamma_1^2 < m_4\lambda_{10}(\gamma_1L_F-\gamma_4). \quad (26)$$

Proof:
To show global stability of the equilibrium E^*, we begin with the following positive definite function, as suggested by (32; 33).

$$Y = \frac{1}{2}(P_i-P_i^*)^2 + \frac{m_1}{2}(P_o-P_o^*)^2 + m_2\left(A-A^*-A^*\ln\frac{A}{A^*}\right) + m_3\left(B-B^*-B^*\ln\frac{B}{B^*}\right) + \frac{m_4}{2}(C-C^*)^2 + m_5\left(F-F^*-F^*\ln\frac{F}{F^*}\right).$$

where, m_1, m_2, m_3, m_4, and m_5 are positive constants. We observed that the function Y is positive definite by showing that $Y(P_i,P_o,A,B,C,F) > 0$ in the interior of Ω and $Y(P_i,P_o,A,B,C,F) = 0$ only at E^*.
Differentiating above equation with respect to time "t" along the solutions of model system (1) and rearranging the terms, we have

$$\frac{dY}{dt} = (P_i-P_i^*)\frac{dP_i}{dt} + m_1(P_o-P_o^*)\frac{dP_o}{dt} + m_2\left(\frac{A-A^*}{A}\right)\frac{dA}{dt} + m_3\left(\frac{B-B^*}{B}\right)\frac{dB}{dt} + m_4(C-C^*)\frac{dC}{dt} + m_5\left(\frac{F-F^*}{F}\right)\frac{dF}{dt}. \quad (27)$$

Differentiating above equation with respect to time "t"

along the solutions of model (1) and rearranging the terms, we have

$$\frac{dY}{dt} = -\Big[a_{11}(P_i-P_i^*)^2 + a_{22}(F-F^*)^2 + a_{33}(A-A^*)^2 + a_{44}(B-B^*)^2 + a_{55}(C-C^*)^2 + a_{66}(F-F^*)^2 + a_{16}(P_i-P_i^*)(F-F^*) + a_{23}(P_o-P_o^*)(A-A^*) + a_{24}(P_o-P_o^*)(B-B^*) + a_{25}(P_o-P_o^*)(C-C^*) + a_{26}(P_o-P_o^*)(F-F^*) + a_{35}(A-A^*)(C-C^*) + a_{56}(C-C^*)(F-F^*)\Big].$$

Where,

$$a_{11} = \mu_1 - \alpha F,$$

$$a_{22} = \left[\frac{m_1\beta_{20}\beta_{21}B}{(\beta_{21}+\beta_{22}P_o^*)(\beta_{21}+\beta_{22}P_o)} + \frac{m_1k_1k_{12}F}{(k_{12}+k_{11}P_o^*)(k_{12}+k_{11}P_o)} + \frac{m_1\beta_{01}\beta_{12}B}{(\beta_{12}+\beta_{11}P_o^*)(\beta_{12}+\beta_{11}P_o)} + m_1\mu_2\right],$$

$$a_{33} = \lambda_{30}, \quad a_{44} = \lambda_{20}, \quad a_{55} = m_4(\gamma_1F-\gamma_4),$$

$$a_{66} = m_5\lambda_{10}, \quad a_{16} = m_5\theta,$$

$$a_{23} = \frac{m_2\lambda_3\beta_1\beta_{12}}{(\beta_{12}+\beta_{11}P_o)(\beta_{12}+\beta_{11}P_o^*)},$$

Where,

$$a_{24} = \frac{m_3\lambda_2\beta_{20}\beta_{21}}{(\beta_{21}+\beta_{22}P_o^*)(\beta_{21}+\beta_{22}P_o)},$$

$$a_{25} = \frac{m_4\beta_{20}\beta_{21}B}{(\beta_{21}+\beta_{22}P_o^*)(\beta_{21}+\beta_{22})},$$

$$a_{26} = \frac{m_5k_1k_{12}}{(k_{12}+k_{11}P_o^*)(k_{12}+k_{11}P_o)},$$

$$a_{56} = m_5\gamma_1 \quad a_{35} = m_4\gamma_2.$$

Sufficient conditions for $\frac{dY}{dt}$ to be negative definite obtained by Sylvester's conditions criteria are 26.
We can now choose positive values of m_1, m_2, m_3, m_4, and m_5 provided that inequalities (26) holds. Thus the time-derivative of Y is negative definite and this result demonstrates the non-linear stability of the coexistence equilibrium.

3 Results and Discussion

To strengthen the analytical results and gain deeper insights into the system's behavior, numerical simulations of system (1) are conducted. It is evident that, with these numerical values, the conditions for local stability (Theorem 1) and global stability (Theorem 26) are satisfied. The values corresponding to the interior equilibrium point of model (1) are

Table 1: The baseline values of the model (1) parameters

Parameters	Baseline Value	Source
Q_1, Q_2	$18.056\ mq/L/day$	(34)
Λ	$16.913\ mq/L/day$	(34)
Λ_1	$0.5\ day^{-1}$	Assumed
Λ_2	$0.5\ day^{-1}$	Assumed
Λ_3	$0.5\ day^{-1}$	Assumed
α	$0.05\ mg/day/fish$	Assumed
θ	$0.02\ fish/day$	Assumed
λ_2	$0.33\ cell/gm$	(34)
λ_3	$0.2\ plants/gm$	Assumed
λ_4	$0.13\ fish/mg$	Assumed
λ_{10}	$0.446\ m^2/fish/day$	(34)
λ_{20}	$8.278\ L/cell/day$	(34)
λ_{30}	$0.5\ L/mg/day$	Assumed
β_{01}	$0.029\ day^{-1}$	(35)
β_{02}	$0.112\ L/cell$	(34)
β_{20}	$4.38\ mq/day/cell$	(25)
β_{11}	11 –	(35)
β_{12}	$1\ mq/L/day$	(35)
β_{21}	$7.81\ mg/L$	(25)
β_{22}	1.48 –	(25)
k_1	$1\ mg/day/fish$	Assumed
k_{11}	1 –	Assumed
k_{12}	$1\ mg/m^2$	Assumed
μ_1	$0.2\ day^{-1}$	Assumed
μ_2	$1.804\ day^{-1}$	(34)
μ_3	$0.031\ day^{-1}$	Assumed
μ_4	$0.3\ day^{-1}$	(34)
μ_5	$1.5\ day^{-1}$	(34)
μ_6	$0.28\ day^{-1}$	(34)
γ_1	$0.1\ fish\ L/m^2/mg$	(34)
γ_2	$0.5\ L/m^2$	Assumed
γ_3	$0.05\ L/cell$	Assumed

$$P_i^* = 43.400, \quad P_o^* = 7.739, \quad A^* = 4.316,$$
$$B^* = 0.098, \quad C^* = 34.220, \quad \text{and} \quad F^* = 4.290.$$

This indicates that the interior equilibrium E^* is locally and globally asymptotically stable for the given parameters. The eigenvalues of the Jacobian matrix corresponding to this interior equilibrium are

$$-0.5661, \quad -0.4095, \quad -1.9870,$$
$$-1.5056, \quad -2.6220+1.8455i, \quad -2.6220-1.8455i.$$

Since all these eigenvalues are either negative or have negative real parts, the interior equilibrium E^* is locally asymptotically stable.

Figures 2(a)–(c) demonstrate that E^* exhibits global stability within the region of attraction defined by the set Ω. These figures illustrate that, for any initial conditions of the considered dynamic variables in the P_i–P_o–F, P_o–C–F, and A–B–F spaces, the solution trajectories converge towards E^*, suggesting the global stability behavior of the interior equilibrium in these spaces.

In Fig. 3(a), the graph demonstrates the relationship between the discharge rate of inorganic pollution (Q_1) and the fish population (F). As the value of Q_1 increases, the fish population F decreases. This indicates that higher levels of inorganic pollution have a detrimental effect on the fish population, leading to a decline in their numbers over time.

In Fig. 3(b), the graph illustrates the relationship between the discharge rate of organic pollution (Q_2) and the fish population (F). In this case, as the value of Q_2 increases, the fish population F also increases, since organic matter serves as a food source for the fish. This suggests that a certain level of organic pollution can potentially promote the growth or sustainability of the fish population.

These findings from Figs. 3(a) and 3(b) highlight the contrasting effects of inorganic and organic pollution on fish population dynamics.

Figs. 4(a) and 4(b) highlight the stimulatory effects of organic pollution on certain aquatic species, such as plants and bacteria, due to the increased availability of organic nutrients. In contrast, Fig. 4(c) emphasizes the potential negative consequences of organic pollution, particularly oxygen depletion, which can adversely affect aquatic ecosystems and the organisms inhabiting them.

In Fig. 4(a), as the discharge rate of organic pollutants (Q_2) increases, there is a corresponding rise in the population of aquatic plants, specifically algae and water hyacinth. This trend indicates that organic pollutants serve as nutrients, promoting the growth and proliferation of these plants in the aquatic environment.

Similarly, Fig. 4(b) shows that an increase in Q_2 leads to bacterial proliferation. Bacteria utilize organic matter as an energy source, and the availability of such matter accelerates bacterial growth, resulting in an overall increase in bacterial populations as organic pollution intensifies.

Conversely, Fig. 4(c) depicts a critical ecological consequence of excessive organic pollution. As Q_2 increases, the concentration of dissolved oxygen in the water decreases. This decline is primarily due to microbial decomposition, during which bacteria consume large amounts of oxygen to break down organic matter. The resulting oxygen depletion can disrupt aquatic ecosystems, potentially leading to hypoxia and eutrophication, both of which pose serious threats to oxygen-dependent aquatic organisms. Generally, Simulation results show that pollutant concentrations

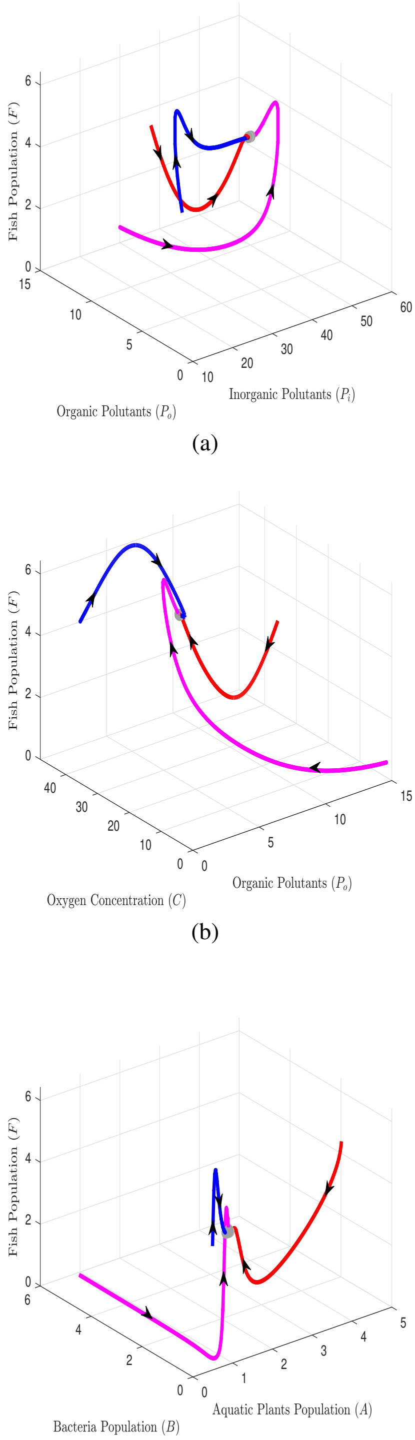

Fig. 2: Nonlinear stability analysis of the co-existence equilibrium (E^*) for a range of parameters in the $P_i - P_o - F$, $P_o - C - F$, and $A - B - F$ planes, as detailed in Table 1.

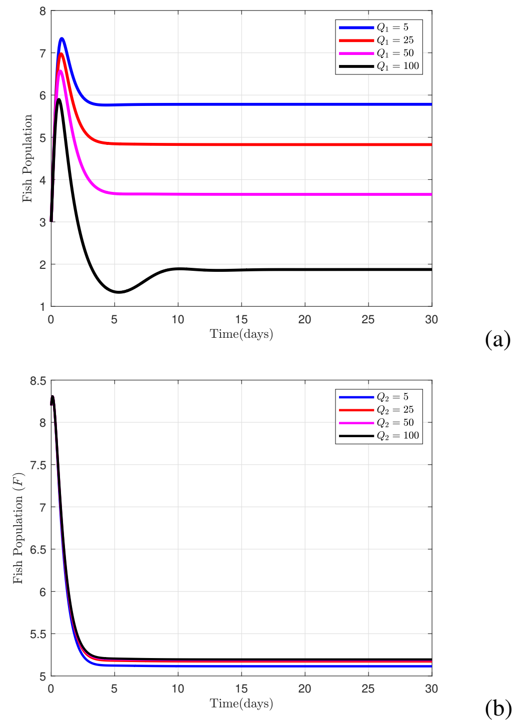

Fig. 3: Effect of discharge rates of (a) inorganic pollutant (Q_1) and (b) organic pollutant (Q_2) on fish population dynamics.

increase rapidly, leading to a significant decline in dissolved oxygen and the fish population. The presence of aquatic plants initially supports oxygen production but later causes oxygen depletion due to decomposition. This confirms the dual role of aquatic vegetation in regulating oxygen dynamics. These findings are consistent with previous models such as those presented by Misra (2011) and Tiwari et al. (2019), which also emphasized the role of algal blooms and bacterial activity in oxygen depletion. However, unlike these studies, our model explicitly incorporates the dual nature of aquatic plants, especially invasive species, showing both their contribution to oxygen production via photosynthesis and their harmful effects through oxygen depletion during decomposition. This added dimension makes our model more ecologically comprehensive. Moreover, while earlier studies primarily concentrated on algal blooms and their linkage to nutrient influx, our model accounts for multiple biological interactions, including fish mortality directly caused by inorganic pollutants and indirectly via oxygen depletion.

3.1 Conclusion

This study investigates the impact of organic and inorganic pollutant discharge rates on the survival of

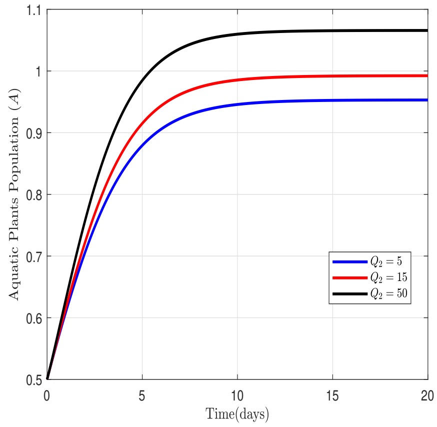

(a) Plant Population

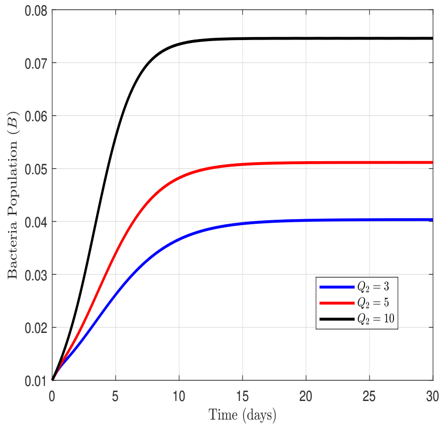

(b) Bacteria Population

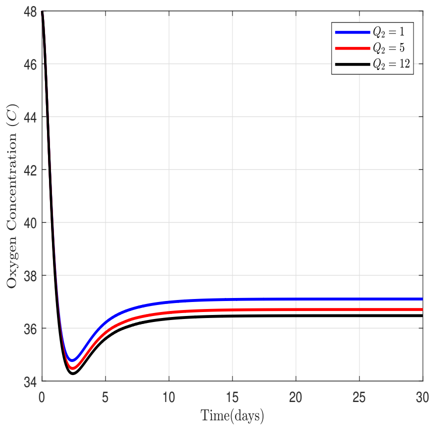

(c) Oxygen Concentration

Fig. 4: Effects of organic pollutant discharge rate (Q_2) on (a) plant population, (b) bacteria population, and (c) oxygen concentration in the ecosystem.

aquatic species, particularly fish, in aquatic environments.

A system of six nonlinear differential equations was developed to model the interactions among organic pollutants, inorganic pollutants, aquatic plants, bacteria, dissolved oxygen, and fish populations. Unlike previous studies, this research incorporates aquatic plants into the system and broadens the scope of interactions, allowing for a more comprehensive understanding of ecosystem dynamics under pollution stress. The study identifies and analyzes four equilibrium points to characterize the system's behavior. The results offer key insights into how different types of pollution affect aquatic ecosystems. Inorganic pollution (Q_1) is associated with a decline in fish populations (F), highlighting its long-term detrimental effects. In contrast, increased organic pollution (Q_2) leads to a rise in fish population (F), suggesting that, under certain conditions, organic pollutants may support fish growth and sustainability. However, excessive organic pollution can deplete dissolved oxygen levels, threatening the survival of aquatic organisms.

These findings underscore the need for effective pollution management strategies to maintain balanced aquatic ecosystems and ensure the health of fish and other species. Understanding these dynamics is vital for informed environmental conservation and policy-making. This study emphasizes the importance of global efforts to reduce harmful chemical discharges into aquatic ecosystems. By limiting pollutant inputs, fish mortality can be mitigated and dissolved oxygen levels preserved—both of which are essential for aquatic life, as discussed in (37; 38). These insights, supported by the model's findings, offer practical strategies for mitigating the adverse effects of pollution on aquatic ecosystems.

Acknowledgement

The first author expresses heartfelt gratitude to the College of Business Education (CBE) for granting study leave, which enabled the pursuit of this academic endeavor. Special appreciation is also extended to the Nelson Mandela African Institution of Science and Technology (NM-AIST) for offering admission and providing a highly conducive studying environment throughout the course of this study.

References

[1] S. Datta, D. Sinha, V. Chaudhary, S. Kar, A. Singh, Water pollution of wetlands: a global threat to inland, wetland, and aquatic phytodiversity: Handbook of research on monitoring and evaluating the ecological health of wetlands, IGI Global, 27-50 (2022).

[2] A. Iyiola, A. Akinrinade, F. Ajayi, Effects of Water Pollution on Biodiversity Along the Coastal Regions, Biodiversity in Africa: Potentials, Threats and Conservation, Springer, 345-367 (2022).

[3] A. Inyinbor, O. Adebesin, P. Oluyori, A. Adelani O. Dada,A. Oreofe,Water pollution: effects, prevention, and climatic impact, Water challenges of an urbanizing world, IntechOpen Rijeka, Croatia, **33**, 33-7 (2018).
[4] J. Shukla, A. Misra, P. Chandra, Mathematical modeling and analysis of the depletion of dissolved oxygen in eutrophied water bodies affected by organic pollutants, Nonlinear Analysis: Real World Applications, Elsevier, **9**, 1851-1865 (2008).
[5] P. Babuji, S. Thirumalaisamy, K. Duraisamy, G. Periyasamy, Human health risks due to exposure to water pollution: a review, Water, MDPI **15**, 2532 (2023).
[6] National Organization for Rare Disorders (NORD), Heavy Metal Poisoning(2024).
[7] W. M. Manetu, A.M. Karanja, Waterborne disease risk factors and intervention practices: a review, Open Access Library Journal, Scientific Research Publishing, **8**, 1-11 (2021).
[8] S. Sahoo, S. Goswami, Theoretical framework for assessing the economic and environmental impact of water pollution: A detailed study on sustainable development of India, Journal of Future Sustainability **4**,23-34 (2024).
[9] J. Shukla, A. Misra,P Chandra, Mathematical modeling of the survival of a biological species in polluted water bodies, Differential Equations and Dynamical Systems, **15**, 209-230 (2007).
[10] S. Siddiqua, A. Chaturvedi, R. Gupta, A Review-Mathematical Modelling on Water Pollution and Its Effects on Aquatic Species, Advances in Applied Mathematics Conference, 835-842 (2020).
[11] F. Adebayo, S. Obiekezie, Microorganisms in waste management, Research Journal of Science and Technology,A&V Publications **10** 28-39 (2018).
[12] A. Ansari, S. Gill, F. Khan, Eutrophication: threat to aquatic ecosystems ,Eutrophication: causes, consequences and control, Springer, 143-170 (2010).
[13] A. Chaturvedi, K. Ramesh, G. Vatsala, A mathematical approach to study the effect of pollutants/toxicants in aquatic environment, International Journal of Research-Granthaalayah**5** 33-38 (2017).
[14] A. Kadam, V. Wagh, B. Umrikar, R. Sankhua, An implication of boron and fluoride contamination and its exposure risk in groundwater resources in semi-arid region, Western India, Environment, development and sustainability, Springer, **22**, 7033-7056 (2020).
[15] V. Sivasankar, A. Darchen, K. Omine, R. Sakthivel, Fluoride: A world ubiquitous compound, its chemistry, and ways of contamination, Surface modified carbons as scavengers for fluoride from water, Springer, 5-32 (2016).
[16] M. Ahmaruzzaman, Industrial wastes as low-cost potential adsorbents for the treatment of wastewater laden with heavy metals, Advances in colloid and interface science, Elsevier **166** 36-59, (2011).
[17] , U. Förstner, G. T. Wittmann, Metal pollution in the aquatic environment, Springer Science & Business Media (2012).
[18] L. Chen, S. Du, D. Song, P. Zhang, L. Zhang, Ecotoxicology of heavy metals in marine fish, Marine Pollution: Current Status, Impacts and Remedies, Bentham Science Publishers, **1** 173-230, (2019).
[19] R. C. Altamirano, A. P. Sierra-Beltrán, Biotoxins from freshwater and marine harmful algal blooms occurring in Mexico,Toxin Reviews, Taylor & Francis **27**, 27-77 (2008).
[20] A. J. King, J. Lieshcke, Short-term effects of a prolonged blackwater event on aquatic fauna in the Murray River, Australia: considerations for future events, Marine and Freshwater Research, CSIRO Publishing, **63**, 576-586 (2012).
[21] R. Vertessy, D. Barma, L. Baumgartner, S. Mitrovic, F. Sheldon, N. Bond, Independent assessment of the 2018–19 fish deaths in the lower Darling, Government of Australia, (2019).
[22] S. Townsend, K. Boland, T. Wrigley, Power and Water Authority, Northern Territory, Citeseer.
[23] C. Marin, Characterization of the striped mullet (Mugil cephalus) in Southwest Florida: Influence of fishers and environmental factors, Florida Gulf Coast University, (2018)
[24] The National Special Committee Appointed by Minister of State in the Vice President's Office – Environment and Union, Report on the Investigation of the Source of Mara River Pollution, (2022).
[25] P. Tiwari, I. Bulai, A. Misra, E. Venturino, Modeling the direct and indirect effects of pollutants on the survival of fish in water bodies, Journal of Biological Systems, World Scientific, **25**, 521-543 (2017).
[26] A. Misra, Modeling the depletion of dissolved oxygen due to algal bloom in a lake by taking Holling type-III interaction, Applied mathematics and computation, Elsevier, **217**, 8367-8376 (2011).
[27] A. Kumar, A. Agrawal, A. Hasan, A. Misra, Modeling the effect of toxicant on the deformity in a subclass of a biological species, Modeling Earth Systems and Environment, Springer, **2** 1-14 (2016).
[28] N. Akhtar, I. Syakir, I. Muhammad, S. Bhawani, K. Umar, Various natural and anthropogenic factors responsible for water quality degradation: A review, Water, MDPI, **13**, 26-60 (2021).
[29] S. Missaghi, M. Hondzo, W. Herb, Prediction of lake water temperature, dissolved oxygen, and fish habitat under changing climate, Climatic Change, Springer, **142**, 747-757 (2017).
[30] A. Misra, P. Chandra, J. Shukla, Mathematical modeling and analysis of the depletion of dissolved oxygen in water bodies, Nonlinear analysis: real world applications, Elsevier, **7**, 980–996, (2006).
[31] A. Jha, A. Misra, A robust role of carbon taxes towards alleviating carbon dioxide: a modeling study, Journal of Engineering Mathematics, Springer, **144**, 20 (2024).

[32] I. Fanuel, S. Mirau, D. Kajunguri, F. Moyo, Conservation of forest biomass and forest-dependent wildlife population: Uncertainty quantification of the model parameters, Heliyon, Elsevier, **9** (2023).
[33] P. Kalra, S. Tangri, Study of effects of toxicants and acidity on oxygen-dependent aquatic population: a mathematical model, International Journal of Mathematical Modelling and Numerical Optimisation, Inderscience Publishers (IEL), **10**, 307-329 (2020).
[34] P. Tiwari, I. Bulai, A. Misra, E. Venturino, Human population effects on the Ulsoor lake fish survival, Journal of Biological Systems, World Scientific, **26** 603-632 (2018).
[35] P. Tiwari, S. Samanta, F. Bona, E. Venturino, A. Misra, The time delays influence on the dynamical complexity of algal blooms in the presence of bacteria, Ecological complexity, Elsevier **39**, 100-769 (2019).
[36] D. Sarma, D. Kumar, Eutrophication in freshwater and its microbial implications, Handbook of Aquatic Microbiology, CRC Press, 194-209 (2024)
[37] A. Bulbul Ali, A. Mishra, Effects of dissolved oxygen concentration on freshwater fish: a review, International Journal of Fisheries and Aquatic Studies, **10**, 113-127 (2022).
[38] F. Kibuye, A. Zamyadi, E. Wert, A critical review on operation and performance of source water control strategies for cyanobacterial blooms: Part II-mechanical and biological control methods, Harmful Algae, Elsevier, **109**, 102-119 (2021).
[39] K. Kasiotis, E. Zafeiraki, E. Manea-Karga, D. Kouretas, F. Tekos, Z. Skaperda, N. Doumpas, K. Machera, Bioaccumulation of Organic and Inorganic Pollutants in Fish from Thermaikos Gulf: Preliminary Human Health Risk Assessment Assisted by a Computational Approach, Journal of Xenobiotics, MDPI **14**, 701-716 (2024).
[40] S. Bunn, P. Davies, M. Winning, Sources of organic carbon supporting the food web of an arid zone floodplain river, Freshwater Biology, Wiley Online Library, **48**, 619-635 (2003).
[41] E. Lipczynska-Kochany, Humic substances, their microbial interactions and effects on biological transformations of organic pollutants in water and soil: A review, Chemosphere, Elsevier, **202**, 420-437 (2018).
[42] M. Jan, S. Hassan, A. Ara, Freshwater Biodiversity: Indicators of Eutrophication and Pollution, Biodiversity of Freshwater Ecosystems, Apple Academic Press, 263-284 (2022).
[43] S. Rathore, P. Chandravanshi, A. Chandravanshi, K. Jaiswal, Impacts of excess nutrient inputs on aquatic ecosystem, IOSR Journal of Agriculture and Veterinary Science, Citeseer **9**, 89-96 (2016).

Christopher Ngalya is a PhD candidate in Mathematical and Computer Science and Engineering at NM-AIST, specializing in applied mathematics and computational sciences. He serves as an Assistant Lecturer at the College of Business Education. He holds a BSc in Education from St. John's University of Tanzania and an MSc from NM-AIST. His research focuses on modeling dynamical systems to address real-world challenges in fields such as ecology, economy, health, education, and technology.

Silas Mirau is a Lecturer in Applied Mathematics and Computational Science at NM-AIST's School of CoCSE. He holds a PhD in Applied Mathematics and Statistics from Beijing Institute of Technology, an MSc in Technomathematics and Technical Physics from LUT, Finland, and a BEd Sc in Mathematics from the University of Dar es Salaam. His research focuses on time series modeling, information geometry, and epidemiology. He has supervised numerous Master's and PhD students and has contributed to various project proposals, including HEI-ICI, DAAD, and WOLIMODs. He currently serves as Deputy Leader of the Mathematical Modeling Research Group and Chief Invigilator at CoCSE.

Maranya Mayengo is a Lecturer in Mathematics at the School of CoCSE, NM-AIST. He began his teaching journey with a Diploma in Education from Monduli Teachers' College (2006), followed by a B.Ed. (Science) from the University of Dodoma (2011). He earned both his Master's and Ph.D. in Applied Mathematics and Computational Science from NM-AIST in 2014 and 2021, respectively. Dr. Mayengo is recognized for his dedication to inclusive education, teacher professional development, and student empowerment. He has led workshops for school teachers on competence-based approaches and is committed to transforming education through innovative, student-centered practices.